

# Supporting Information

## **Chemically Driven Superstructural Ordering Leading to Giant Unit Cells in Unconventional Clathrates Cs<sub>8</sub>Zn<sub>18</sub>Sb<sub>28</sub> and Cs<sub>8</sub>Cd<sub>18</sub>Sb<sub>28</sub>**

Bryan Owens-Baird,<sup>1,2</sup> Philip Yox,<sup>1,2,3</sup> Shannon Lee,<sup>1,2</sup> Xian B. Carroll,<sup>4</sup> Suyin Grass Wang,<sup>5</sup> Yu-Sheng Chen,<sup>5</sup> Oleg I. Lebedev,<sup>3</sup> Kirill Kovnir<sup>1,2,\*</sup>

<sup>1</sup> *Department of Chemistry, Iowa State University, Ames, IA 50011, USA*

<sup>2</sup> *Ames Laboratory, U.S. Department of Energy, Ames, IA 50011, USA*

<sup>3</sup> *Laboratoire CRISMAT, UMR 6508, CNRS-ENICAEN, Caen 14050, France*

<sup>4</sup> *Department of Chemistry, University of Tennessee, Knoxville, TN 37996, USA*

<sup>5</sup> *NSF's ChemMatCARS, Center for Advanced Radiation Source, The University of Chicago, Argonne, USA*

E-mail: [kovnir@iastate.edu](mailto:kovnir@iastate.edu)

### **Powder X-ray Diffraction**

Samples were analyzed via room-temperature powder X-ray diffraction using a Rigaku Miniflex 600 diffractometer employing Cu- $K_\alpha$  radiation ( $\lambda = 1.54185 \text{ \AA}$ ) with a Ni- $K_\beta$  filter. Scans were performed from  $5\text{--}80^\circ 2\theta$  on a spinning Si-crystal zero-background plate on air.

### **High-Resolution Synchrotron Powder X-ray Diffraction**

High-resolution synchrotron PXRD datasets were collected from beamline 11-BM at the Advanced Photon Source at Argonne National Lab (APS ANL). A wavelength of  $0.412748 \text{ \AA}$  was employed and the samples were housed in Kapton capillaries.

### **Variable Temperature Synchrotron Powder X-ray Diffraction**

Variable temperature PXRD data was collected at the synchrotron beamline 17-BM at the APS ANL. Samples were loaded into  $0.5 \text{ mm}$  inner diameter silica capillaries ( $0.7 \text{ mm}$  outer diameter) and sealed under vacuum. The sealed silica capillaries were placed into a secondary shield capillary, with a thermocouple set as close as possible to the measurement area. An experimental set-up can be found elsewhere.<sup>1</sup> The data were collected with  $\lambda = 0.24125 \text{ \AA}$  and a temperature range from  $300 \text{ K}$  to  $997 \text{ K}$ . Temperature calibration of the setup was achieved by measurement of Sn, Sb, and Ge powders loaded into capillaries and melted; melting points of the standards were compared to literature melting points.

### **Single-Crystal X-ray Diffraction**

In-house Single-Crystal X-ray Diffraction was carried out using a Bruker D8 Venture diffractometer with a Bruker Photon100 CMOS detector employing Mo- $K_\alpha$  radiation ( $\lambda = 0.71073 \text{ \AA}$ ). The dataset was collected at  $100 \text{ K}$  under a  $\text{N}_2$  stream with a variety of  $\varphi$ - and  $\omega$ -scans recorded at a  $0.3^\circ$  step and integrated using the Bruker SAINT software package.<sup>2</sup> Multiscan absorption correction was used.

Synchrotron Single-Crystal X-ray diffraction experiments for  $\text{Cs}_8\text{Cd}_{18}\text{Sb}_{28}$  crystals were carried out at 15-ID at the APS ANL. The data was collected with a wavelength of  $0.24797 \text{ \AA}$  at a temperature of  $10 \text{ K}$  under a flowing stream of He using a  $\varphi$ -scan recorded at  $0.2^\circ$  steps. Identical data workup procedures were used to the in-house procedures above. The dataset for  $\text{Cs}_8\text{Cd}_{18}\text{Sb}_{28}$  clathrate was collected up to high  $\sin\theta/\lambda = 1.19 \text{ \AA}^{-1}$  and data/param ratio of 133. Synchrotron Single-Crystal X-ray diffraction experiments for  $\text{Cs}_8\text{Zn}_{18}\text{Sb}_{28}$  crystals were carried out at beamline 11.3.1 at the Advanced Light Source, Lawrence Berkeley Laboratory ( $\lambda = 0.7749 \text{ \AA}$ ). The crystal was mounted in the  $100 \text{ K}$  nitrogen cold stream provided by an Oxford Cryostream low temperature apparatus on the goniometer head of a Bruker D8 diffractometer equipped with a Bruker Photon CMOS detector.

Structure solution and refinement was achieved using the SHELX suite.<sup>3</sup> Full details of the structure refinement, atomic positions, occupancy, and atomic displacement parameters can be found in Tables S1-S4. For refinement of the  $\text{Cs}_8\text{Zn}_9\text{Cd}_9\text{Sb}_{28}$  structure (in-house instrument), sump commands were employed to constrain the relative ratios of Zn, Cd, and Sb over the three framework positions. The total sum of Zn, Cd, and Sb was constrained to 46 atoms, the number of atoms within the type-I clathrate archetype cell. Then the relative ratio between Zn and Cd was artificially shifted to slightly Zn- and Cd-rich compositions and refined and  $R_1$  values compared. The best refinement results came from the model in which Zn and a Cd composition were equal and is the solution presented.

## Scanning Electron Microscopy and Energy Dispersive X-ray Spectroscopy

Elemental composition analysis was performed through Energy Dispersive X-ray Spectroscopy using a FEI Quanta 250 field emission-SEM with EDS detection (Oxford X-Max 80) and Aztec software. For each composition, measurements were taken at a collection of sites on multiple crystals to improve statistics.

## Transmission Electron Microscopy

High-resolution TEM (HRTEM) and electron diffraction (ED) studies were performed using a Tecnai G2 30 UT (LaB<sub>6</sub>) microscope operated at 300 kV with 0.17 nm point resolution and equipped with an EDAX EDX detector. High angle annular dark field (HAADF)–scanning TEM (STEM) and annular bright field scanning TEM (ABF-STEM) studies were performed using a JEM ARM200F cold FEG double aberration corrected electron microscope operated at 200 kV and equipped with a large solid-angle CENTURIO EDX detector and Quantum EELS spectrometer.

## Differential Scanning Calorimetry

Differential Scanning Calorimetry was performed using a 404 F1 Pegasus calorimeter (Netzsch Thermal Analysis). Approximately 30 mg of sample was loaded in silica ampoules, which were evacuated and sealed. The DSC measurements were performed between 300-1020 K with a heating/cooling rate of 10 K/min.

## Sample Densification

Pellets of Cs<sub>8</sub>Zn<sub>18-x</sub>Cd<sub>x</sub>Sb<sub>28</sub> ( $x = 0, 4.5, 9, 13.5, 18$ ) for property measurements were prepared by spark plasma sintering (Dr. Sinter Lab Jr. 211 Lx). Finely ground powders were loaded into a 5 mm diameter graphite die with tungsten carbide plungers. Samples of Cs<sub>8</sub>Zn<sub>18-x</sub>Cd<sub>x</sub>Sb<sub>28</sub> ( $x = 0, 4.5, 9, 13.5$ ) were sintered through the application of a uniaxial pressure of 156 MPa and a temperature of 673 K for 10 min. Pellets of Cs<sub>8</sub>Cd<sub>18</sub>Sb<sub>28</sub> using this heating profile were fragile and easily broken, instead a dwell time of 20 min was used to produce more robust pellets. The pelletized samples of Cs<sub>8</sub>Zn<sub>18-x</sub>Cd<sub>x</sub>Sb<sub>28</sub> ( $x = 0, 4.5, 9, 13.5, 18$ ) had densities of 96%, 94%, 98%, 97%, and 98% of their theoretical X-ray densities, respectively. These densities were determined by both geometrical and Archimedes-based methods. Phase-purity of the pellets after pressing was confirmed through PXRD.

## Transport Properties

Thermal and charge-transport properties were measured from 10-300 K using a Quantum Design Physical Property Measurement System. The Seebeck thermopower and thermal conductivity were measured using the Thermal Transport Option in a two-probe configuration. Electrical resistivity was measured using the Alternating Current Transport option and a four-probe geometry with 50  $\mu$ m platinum wires and silver paste.

1. P. J. Chupas, K. W. Chapman, C. Kurtz, J. C. Hanson, P. L. Lee, C. P. Grey, *J. Appl. Crystallogr.* **2008**, 41 (4), 822-824.
2. W. Bruker AXS Inc.: Madison, USA, **2007**.
3. G. Sheldrick, *Acta Crystallographica Section A* **2008**, 64 (1), 112-122.

**Table S1.** Single crystal data and refinement parameters of Cs<sub>8</sub>Cd<sub>18</sub>Sb<sub>28</sub> and Cs<sub>8</sub>Zn<sub>9</sub>Cd<sub>9</sub>Sb<sub>28</sub>.

empirical formula	Cs <sub>7.95</sub> Cd <sub>18</sub> Sb <sub>27.99</sub>	Cs <sub>8</sub> Zn <sub>9</sub> Cd <sub>9</sub> Sb <sub>28</sub>
formula weight	6495.92 g/mol	6072.21 g/mol
temperature	10(2) K	100(2) K
radiation, wavelength	synchrotron, 0.24797 Å	Mo-K <sub>α</sub> , 0.71073 Å
crystal system	cubic	cubic
space group	<i>Ia</i> $\bar{3}d$ (No. 230)	<i>Pm</i> $\bar{3}n$ (No. 223)
unit cell dimensions	<i>a</i> = 24.3160(5) Å	<i>a</i> = 11.9595(7) Å
unit cell volume	14377.3(9) Å <sup>3</sup>	1710.6(3) Å <sup>3</sup>
<i>Z</i>	8	1
Data/parameters	6898/52	498/25
density (calc.)	6.00 g/cm <sup>3</sup>	5.90 g/cm <sup>3</sup>
absorption coefficient	6.39 mm <sup>-1</sup>	20.84 mm <sup>-1</sup>
<i>R</i> <sub>int</sub>	0.05	0.04
goodness-of-fit	1.27	1.11
final <i>R</i> indices [ <i>I</i> > 2σ( <i>I</i> )]	<i>R</i> <sub>1</sub> = 0.012	<i>R</i> <sub>1</sub> = 0.029
	<i>wR</i> <sub>2</sub> = 0.026	<i>wR</i> <sub>2</sub> = 0.042
final <i>R</i> indices [all data]	<i>R</i> <sub>1</sub> = 0.014	<i>R</i> <sub>1</sub> = 0.045
	<i>wR</i> <sub>2</sub> = 0.030	<i>wR</i> <sub>2</sub> = 0.049
largest peak and hole	1.37/-2.17 e Å <sup>-3</sup>	1.26/-1.56 e Å <sup>-3</sup>

**Table S2.** Atomic coordinates and equivalent isotropic displacement parameters of Cs<sub>8</sub>Cd<sub>18</sub>Sb<sub>28</sub> at 10 K.

Atom	Wyckoff site	$x/a$	$y/b$	$z/c$	Occupancy	$U_{eq} (\text{\AA}^2)^a$
Cs1	16a	0	0	0	0.975(1)	0.003(1)
Cs2	48g	0.74743(4)	0.00257(4)	$\frac{3}{8}$	0.790(8)	0.006(1)
Cs22	96h	0.12321(7)	0.74933(5)	0.00623(11)	0.105(2)	0.006(1)
Sb1	24d	$\frac{7}{8}$	0	$\frac{1}{4}$	1	0.002(1)
Cd2	24c	$\frac{1}{8}$	0	$\frac{1}{4}$	1	0.003(1)
Sb3	96h	0.90702(2)	0.08949(2)	0.90741(2)	1	0.002(1)
Sb4	96h	0.05666(2)	0.99973(2)	0.15585(2)	1	0.003(1)
Cd5	96h	0.93913(2)	0.99810(2)	0.15619(2)	1	0.003(1)
Sb61	32e	0.08794(7)	$x$	$x$	0.222(1)	0.004(1)
Sb62	32e	0.08030(2)	$x$	$x$	0.025(1)	0.004(1)
Cd63	32e	0.09147(2)	$x$	$x$	0.75	0.004(1)

<sup>a</sup> $U_{eq}$  is defined as one third of the trace of the orthogonalized  $U_{ij}$  tensor

**Table S3.** Anisotropic displacement parameters ( $\text{\AA}^2$ ) for Cs<sub>8</sub>Cd<sub>18</sub>Sb<sub>28</sub> at 10 K.\*

Atom	$U_{11}$	$U_{22}$	$U_{33}$	$U_{12}$	$U_{13}$	$U_{23}$
Cs1	0.003(1)	0.003(1)	0.003(1)	0.0007(1)	0.0007(1)	0.0007(1)
Cs2	0.007(1)	0.007(1)	0.003(1)	0.0007(1)	0.0000(1)	0.0000(1)
Cs22	0.007(1)	0.007(1)	0.003(1)	0.0007(1)	0.0000(1)	0.0000(1)
Sb1	0.003(1)	0.002(1)	0.002(1)	0	0	0
Cd2	0.003(1)	0.003(1)	0.003(1)	0	0	0.0000(1)
Sb3	0.003(1)	0.002(1)	0.002(1)	0.0003(1)	0.0000(1)	0.0001(1)
Sb4	0.002(1)	0.002(1)	0.003(1)	0.0002(1)	0.0000(1)	0.0000(1)
Cd5	0.003(1)	0.003(1)	0.003(1)	0.0002(1)	0.0007(1)	0.0001(1)
Sb61	0.004(1)	0.004(1)	0.004(1)	0.0009(1)	0.0009(1)	0.0009(1)
Sb62	0.004(1)	0.004(1)	0.004(1)	0.0009(1)	0.0009(1)	0.0009(1)
Cd63	0.004(1)	0.004(1)	0.004(1)	0.0009(1)	0.0009(1)	0.0009(1)

\*The anisotropic displacement factor exponent takes the form:  $-2\pi^2[h^2a^{*2}U_{11} + \dots + 2hka^*b^*U_{12}]$ .

**Table S4.** Atomic coordinates and equivalent isotropic displacement parameters of Cs<sub>8</sub>Zn<sub>9</sub>Cd<sub>9</sub>Sb<sub>28</sub> at 100 K.

Atom	Wyckoff site	$x/a$	$y/b$	$z/c$	Occupancy	$U_{eq} (\text{\AA}^2)^a$
Cs1	2a	0	0	1/2	1	0.007(1)
Cs2	6c	1/2	1/4	0	1	0.018(1)
Sb3	6d	1/2	0	1/4	0.48(6)	0.010(1)
Zn3	6d	1/2	0	1/4	0.17(3)	0.010(1)
Cd3	6d	1/2	0	1/4	0.35(7)	0.010(1)
Sb4	16i	0.18294(3)	$x$	$x$	0.82(3)	0.008(1)
Zn4	16i	0.18294(3)	$x$	$x$	0.12(2)	0.008(1)
Cd4	16i	0.18294(3)	$x$	$x$	0.07(3)	0.008(1)
Sb5	24k	0.31204(5)	0	0.11669(5)	0.50(2)	0.009(1)
Zn5	24k	0.31204(5)	0	0.11669(5)	0.25(2)	0.009(1)
Cd5	24k	0.31204(5)	0	0.11669(5)	0.25(2)	0.009(1)

<sup>a</sup> $U_{eq}$  is defined as one third of the trace of the orthogonalized  $U_{ij}$  tensor

**Table S5.** Anisotropic displacement parameters ( $\text{\AA}^2$ ) for Cs<sub>8</sub>Zn<sub>9</sub>Cd<sub>9</sub>Sb<sub>28</sub> at 100 K.\*

Atom	$U_{11}$	$U_{22}$	$U_{33}$	$U_{12}$	$U_{13}$	$U_{23}$
Cs1	0.007(1)	0.007(1)	0.007(1)	0	0	0
Cs2	0.024(1)	0.007(1)	0.024(1)	0	0	0
Sb3	0.009(1)	0.009(1)	0.013(1)	0	0	0
Zn3	0.009(1)	0.009(1)	0.013(1)	0	0	0
Cd3	0.009(1)	0.009(1)	0.013(1)	0	0	0
Sb4	0.008(1)	0.008(1)	0.008(1)	-0.0005(1)	-0.0005(1)	-0.0005(1)
Zn4	0.008(1)	0.008(1)	0.008(1)	-0.0005(1)	-0.0005(1)	-0.0005(1)
Cd4	0.008(1)	0.008(1)	0.008(1)	-0.0005(1)	-0.0005(1)	-0.0005(1)
Sb5	0.007(1)	0.008(1)	0.012(1)	0	0.0001(3)	0
Zn5	0.007(1)	0.008(1)	0.012(1)	0	0.0001(3)	0
Cd5	0.007(1)	0.008(1)	0.012(1)	0	0.0001(3)	0

\*The anisotropic displacement factor exponent takes the form:  $-2\pi^2[h^2a^{*2}U_{11} + \dots + 2hka^*b^*U_{12}]$ .

**Table S6.** Average EDX compositions for  $\text{Cs}_8(\text{Zn}_{1-x}\text{Cd}_x)_{18}\text{Sb}_{28}$  ( $x = 0, 0.25, 0.5, 0.75, 1$ ) samples. Compositions are normalized to 8 Cs for clarity.

Target Composition	Average EDX Composition
$\text{Cs}_8\text{Zn}_{18}\text{Sb}_{28}$	$\text{Cs}_8\text{Zn}_{18.0(3)}\text{Sb}_{28.7(6)}$
$\text{Cs}_8\text{Zn}_{13.5}\text{Cd}_{4.5}\text{Sb}_{28}$	$\text{Cs}_8\text{Zn}_{15.0(9)}\text{Cd}_{5.1(7)}\text{Sb}_{28.6(3)}$ (Zn/Cd = 75/25)
$\text{Cs}_8\text{Zn}_9\text{Cd}_9\text{Sb}_{28}$	$\text{Cs}_8\text{Zn}_{9.0(3)}\text{Cd}_{8.7(4)}\text{Sb}_{27.4(6)}$ (Zn/Cd = 51/49)
$\text{Cs}_8\text{Zn}_{4.5}\text{Cd}_{13.5}\text{Sb}_{28}$	$\text{Cs}_8\text{Zn}_{5.1(4)}\text{Cd}_{14.8(6)}\text{Sb}_{28.4(4)}$ (Zn/Cd = 26/74)
$\text{Cs}_8\text{Cd}_{18}\text{Sb}_{28}$	$\text{Cs}_8\text{Cd}_{18.6(7)}\text{Sb}_{27.8(3)}$

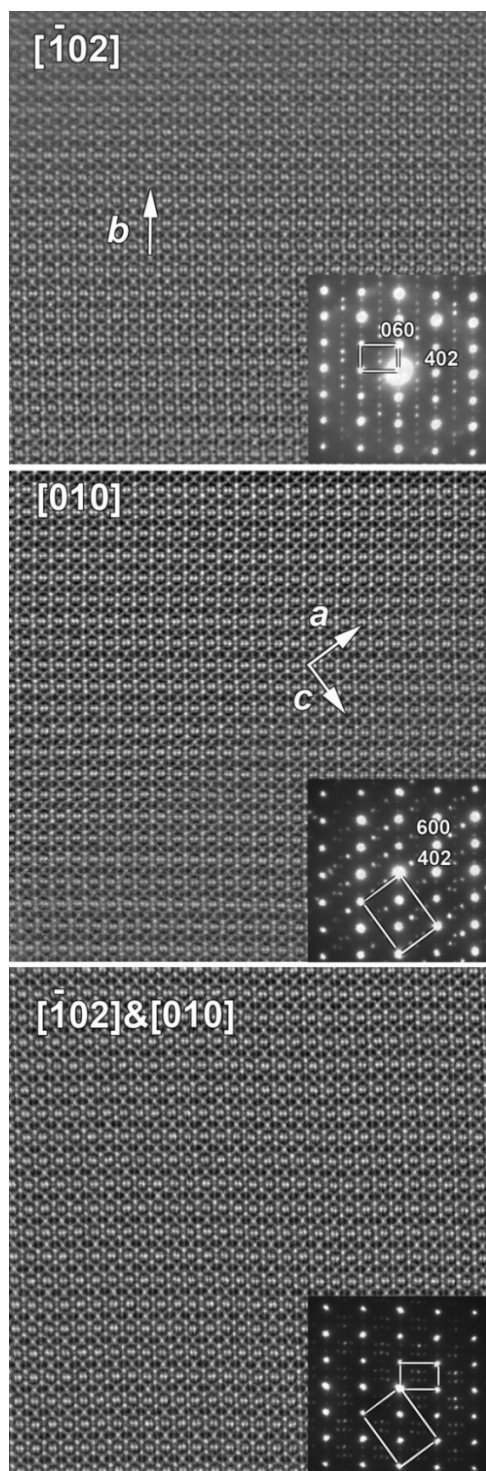


**Figure S1.** HAADF-STEM images illustrated twinning character of  $\text{Cs}_8\text{Zn}_{18}\text{Sb}_{28}$  crystallites: (top) the  $[\bar{1}02]$  HAADF-STEM image and corresponding ED pattern; (middle) the  $[010]$  HAADF-STEM image and corresponding ED pattern; and (bottom) superimposed  $[\bar{1}02]$  and  $[010]$  HAADF-STEM image and ED pattern. The small and large rectangles in the bottom ED pattern indicates the cells of  $[\bar{1}02]$  and  $[010]$ , respectively.



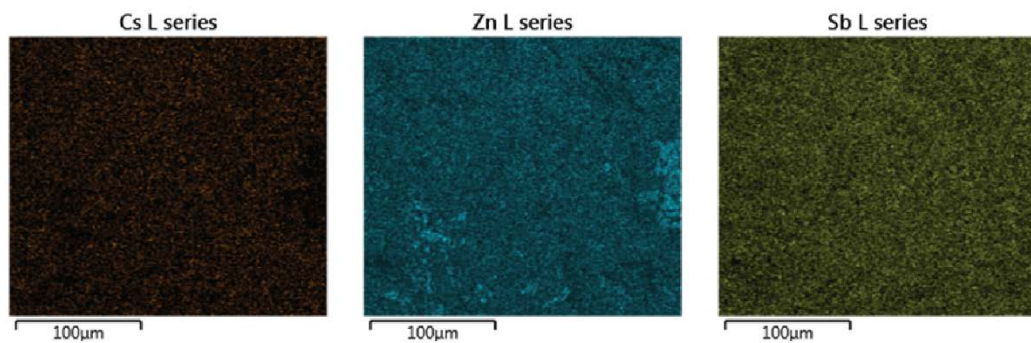


**Figure S2.** SEM-EDX mapping of  $\text{Cs}_8\text{Zn}_{18}\text{Sb}_{28}$  pellet for Cs, Zn, and Sb.

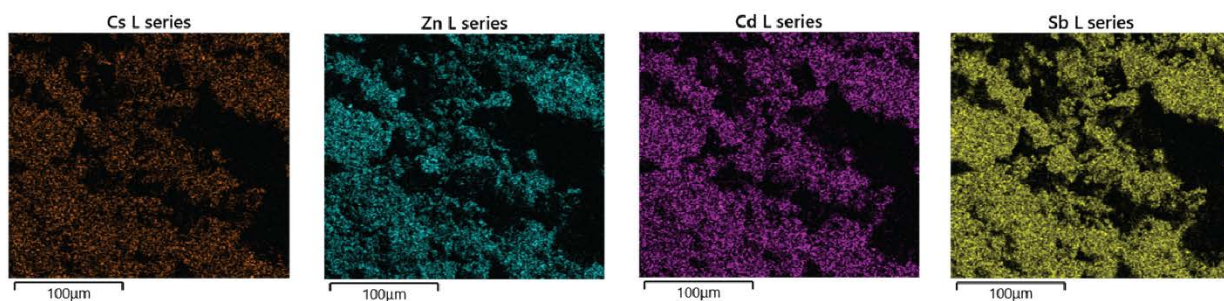


**Figure S3.** SEM-EDX mapping of  $\text{Cs}_8\text{Zn}_9\text{Cd}_9\text{Sb}_{28}$  powder for Cs, Zn, Cd, and Sb. The black regions on the maps are between sample crystallites.

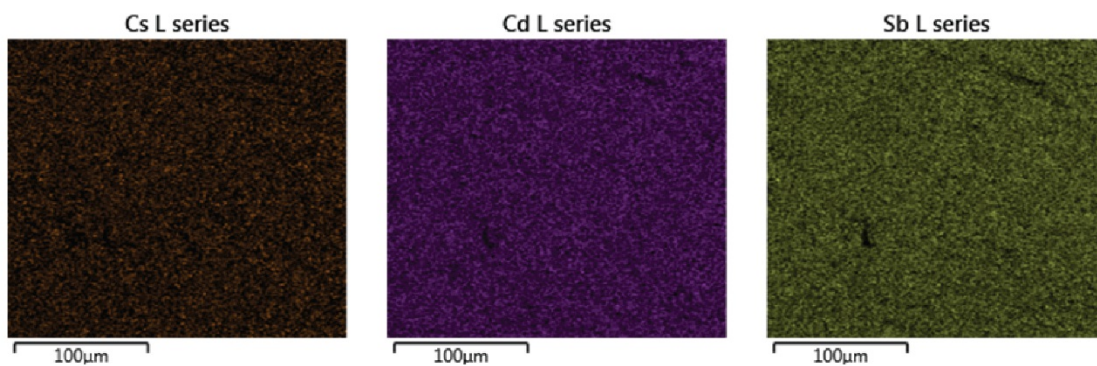


**Figure S4.** SEM-EDX mapping of  $\text{Cs}_8\text{Cd}_{18}\text{Sb}_{28}$  pellet for Cs, Cd, and Sb.

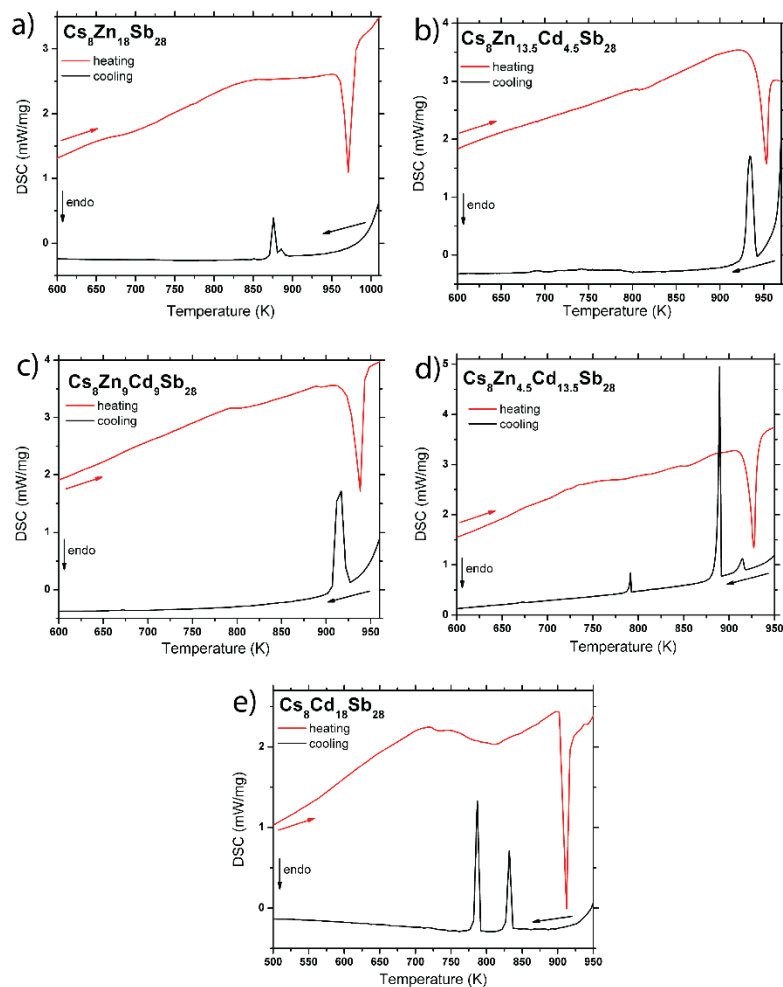


**Figure S5.** DSC plots for  $\text{Cs}_8\text{Zn}_{18-x}\text{Cd}_x\text{Sb}_{28}$  ( $x = 0, 4.5, 9, 13.5, 18$ ). The unlabeled arrows indicate the direction of measurement: red curve for heating and black curve for cooling.

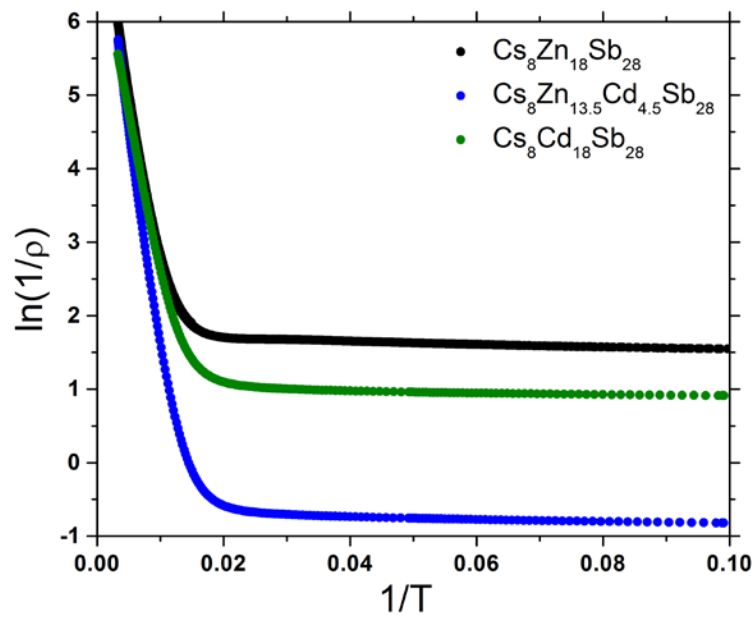


**Figure S6.** Plot of  $\ln(1/\rho)$  vs.  $1/T$  for  $\text{Cs}_8\text{Zn}_{18-x}\text{Cd}_x\text{Sb}_{28}$  ( $x = 0, 4.5, 9$ ).

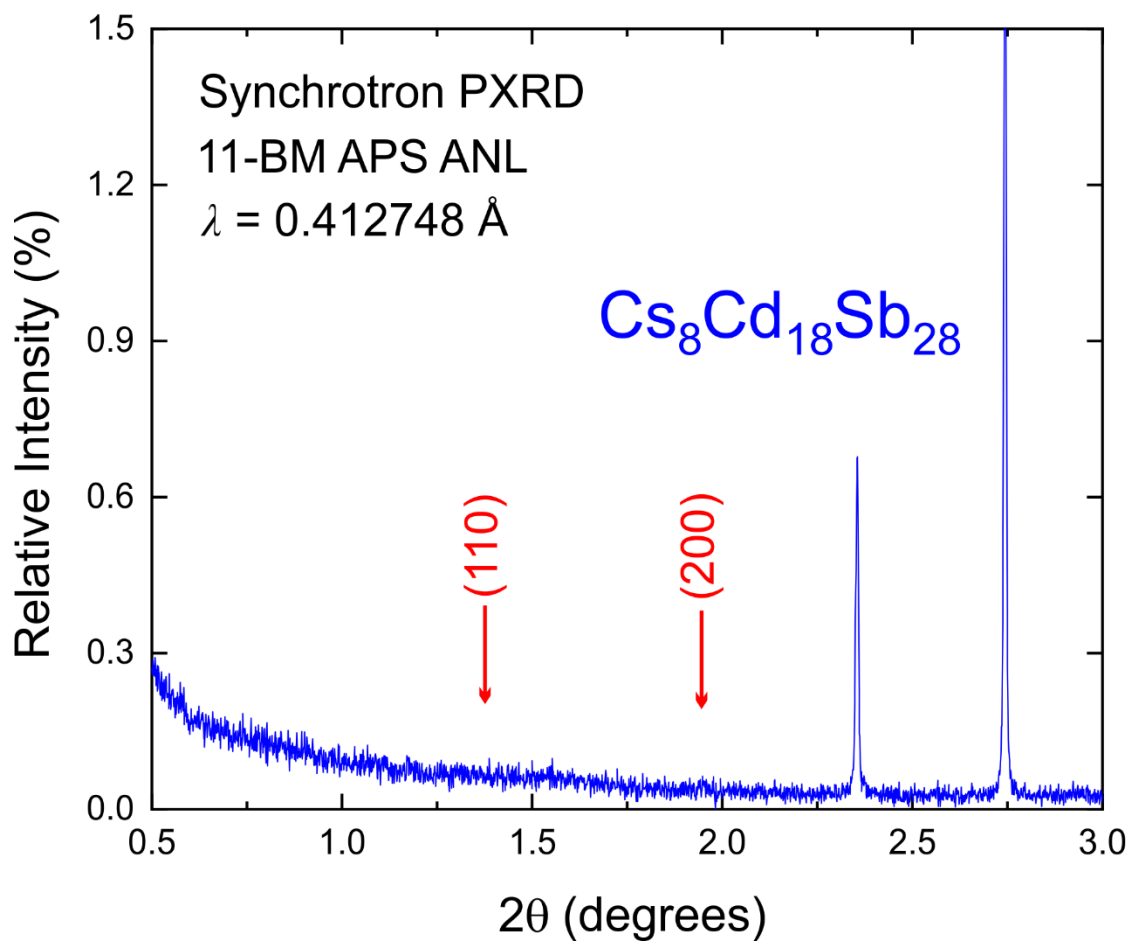


**Figure S7.** A zoomed fragment of the synchrotron powder diffraction pattern for  $\text{Cs}_8\text{Cd}_{18}\text{Sb}_{28}$ . Red arrows indicate the expected location of the observed by electron diffraction reflections (110) and (200).